

Deep *UBVRI* photometry in IC 348^{*,**}

E. Trullols^{1,2} and C. Jordi²

¹ Departament de Matemàtica Aplicada i Telemàtica, Universitat Politècnica de Catalunya, Avda. Victor Balaguer s/n, E-08800 Vilanova i la Geltrú, Spain

² Departament d'Astronomia i Meteorologia, Universitat de Barcelona, Avda. Diagonal 647, E-08028 Barcelona, Spain

Received 5 August 1996 / Accepted 10 December 1996

Abstract. Deep *UBVRI*-CCD Johnson photometry for 123 stars in the densest region of IC 348 open cluster were obtained during three observational runs (October 1992, December 1993 and December 1994) at Calar Alto (Almería, Spain). Colour-colour and colour-magnitude diagrams allowed us to classify 114 stars as members of the cluster and to confirm a large presence of pre-main sequence stars. Individual reddening values were computed for the brightest members. The structure and sub-clustering were discussed and a new sub-cluster was identified. On the assumption that all the stars in the cluster were born at the same time, an age of 3–7 10^6 yr was derived from PMS evolutionary models for low mass stars.

Key words: open clusters and associations: individual: IC 348 – stars: fundamental parameters – stars: pre-main sequence – HR diagram

1. Introduction

The young open cluster IC 348 (C0341+321) is located in the eastern part of the Perseus dark cloud complex, south of the bright star α Persei. Most of the cluster is embedded in warm dust and gas and it is only viewed through a partially transparent region between two dark clouds near the centre of Perseus OB2 association. Using Vilnius photometry Černis (1993) studied the relationship between interstellar extinction and distance, postulating two absorbing dust layers in the direction of IC 348. The first layer, ($A_v = 0.71 \pm 0.27$) at 160 ± 20 pc, covers the whole area of the cluster and is probably related with the Taurus dark cloud complex. The second layer, ($A_v = 2.0 \pm 0.6$) at 260 ± 20 pc has the form of a chain of condensations named

L 1468, L 1470 and L 1471; IC 348 is physically associated with L 1470. The bright stars illuminate surrounding dust and gas forming a group of reflection nebulae, the best known associated with the brightest star BD+31°643 of B5 V spectral type. Dark clouds in the region were analysed in radio wavelengths by Sancisi et al. (1974), Bachiller & Cernicharo (1986) and Bachiller et al. (1987). IRAS sources in the area were studied by Ladd et al. (1993).

The first studies in the region were carried out by Gingrich (1922), Hubble (1922) and Greenstein (1948). In 1952, Blaauw pointed out that the cluster could be a part of the Perseus OB2 association. Harris et al. (1954) observed the central part of IC 348 and obtained *UBV* photometry of 12 stars and spectra of 8 of them, thus allowing the MK classification. Strom et al. (1974) performed *UBVHKL* measurements in a larger area which included some embedded stars, suggesting that the visible cluster may represent only a small part of the group. Herbig (1954) detected 16 H_α emission stars in the IC 348 region that could be classified as PMS stars.

Recently, Lada & Lada (1995) observed the region in the near infrared *JHK*, covering an area of 385 square arc minutes, and estimated a total of 380 star members, 20% of them with infrared excess. They also identified 8 small sub-clusters (each one contained 10–20 stars in a radius of 0.1–0.2 pc) outside the half-mass radius of the cluster. From comparison with the stellar evolutionary models (containing PMS stars) and their observations, they conclude that star formation in IC 348 has been a continuous process over the last 5–7 10^6 yr. Former evaluations of the age, made by Strom et al. (1974), range from 5 to 20 10^6 yr.

The paper by Preibisch et al. (1996) reports the first X-ray analysis of the cluster. They detected 116 sources in very deep pointings with ROSAT PSPC and HRI. Apart from previously known members, they considered as probable cluster members all the H_α emission line stars and 56 additional X-ray sources. The observations by Lada & Lada (1995) were used to estimate individual extinctions of the sources and hence X-ray luminosities. The derived properties of the sources detected were rather similar to those of other young clusters. The authors also conclude that the ionization fraction of the molecular cloud can

Send offprint requests to: E. Trullols

* Based on observations made at the Centro Astronómico Hispano-Alemán and the Observatorio Astronómico Nacional in Calar Alto, Almería, Spain

** Tables 3 and 5 are only available in electronic form from CDS via anonymous ftp 130.79.128.5, and by e-mail request to E. Trullols at enric@mat.upc.es

be considerably enhanced by the X-ray sources, and so they influence the evolution of the cluster.

Historically, clusters have provided important information about the process of star formation and the initial mass function (IMF) because they are statistically significant groups of stars assumed to have a common origin. However, mass segregation and evaporation of low mass members make the determination of the IMF uncertain since a significant fraction of the initial mass can be lost in the process of emerging from molecular clouds in which the stars are formed. So the observations of very young embedded clusters are crucial in IMF determinations.

In this paper we report *UBVRI*-CCD observations of the central region of IC 348 down to visual magnitude 21. These observations are analysed in order to determine individual stellar relationship to the cluster, and faint members are identified. The structure and sub-clustering in the densest region of IC 348 are analysed. A redetermination of the age of the cluster is performed using recent PMS evolutionary models on the assumption that all the stars were born at the same time.

2. Observations and reduction

Deep *UBVRI* Johnson-Cousins CCD photometry was carried out at Calar Alto (Almería, Spain) in October 1992, December 1993 and December 1994 using the 2.20 m telescope of the Centro Astronómico Hispano-Alemán (CAHA), the 1.52 m telescope of the Observatorio Astronómico Nacional (OAN) and the 1.23 m telescope of CAHA, respectively. A TEK#6 chip was used in the CAHA telescopes and a coated THK 31156 in the OAN telescope. Both chips have 1024×1024 pixels, being the pixel size $0.28''$ at 2.20 m, $0.33''$ at 1.52 m and $0.502''$ at 1.23 m telescopes. In the first run we took three overlapping frames in the central region of IC 348, in the second run we re-observed one of these frames, and finally, in the last run, because the chip area was bigger than former, we obtained new frames, each one covering most of the three overlapping frames of the first run. The number of observed frames, exposure times and seeing are given in Table 1. Additional shorter exposures were taken to avoid saturation of brightest stars. Dome flat frames were obtained to normalise the response of each pixel.

About 20 different Landolt's (1983, 1992) standard stars, covering a wide range of spectral types, were also observed each night in order to reproduce the Johnson-Cousins *UBVRI* system.

The reduction from raw images to standard photometry was performed following Jordi et al. (1995). We refer readers to this for a fully detailed description of the procedure.

Bias level was evaluated individually for each frame by averaging the counts of the most stable pixels in the overscan areas. Bias and dark current were subtracted from the frames. As pointed out in previous papers (Galadí-Enríquez et al. 1994, Jordi et al. 1995), the way the shutter opens and closes affects both the images and the flat-fielding process. The shutters of the TEK#6 at 2.20 m and 1.23 m telescopes and the THK 31156 at 1.52 m telescope were analysed following Galadí-Enríquez et

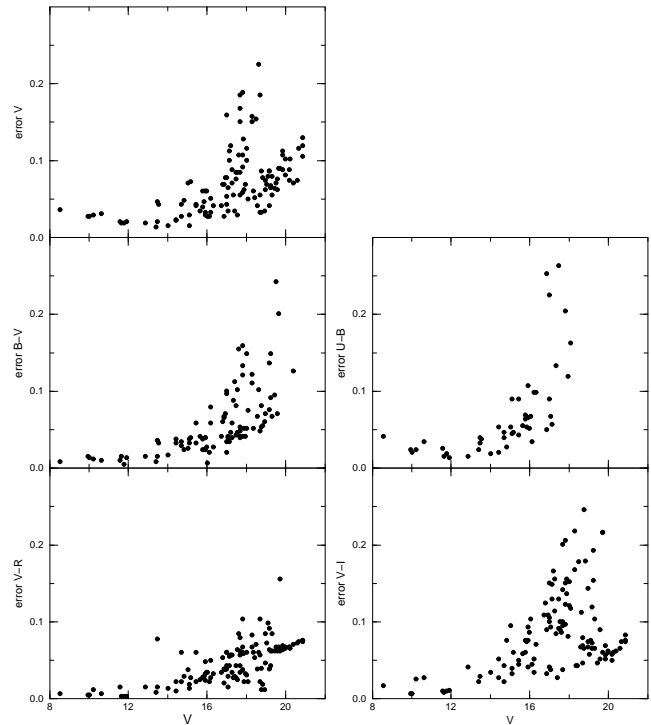


Fig. 1. Internal errors as a function of apparent visual magnitude

al. (1994) and shutter effects were removed from flat-field and object frames.

The frames were processed using the ESO image processing software MIDAS running in an IBM AIX6000 Mod. 540. Aperture photometry and growth curves were obtained using the DAOPHOT and DAOGROW programs (Stetson 1987, 1990). Cross identification of stars in different frames was performed using the DAOMATCH and DAOMASTER programs (Stetson 1993).

The coefficients of the transformation to the standard system were computed by a least square method using the instrumental magnitudes of the standard stars and their standard magnitudes and colours in the Johnson-Cousins system. Standard stars with residuals greater than 2σ were rejected. Transformation to the standard system was performed in two steps, determining first the extinction coefficients (equations (2) and (3) in Jordi et al. (1995)). Independent reductions were made for each night, which gave at least two independent measurements (different telescopes and different chips) for most of the stars. The r.m.s. residuals of the standard stars are given in Table 2.

Internal errors of individual measurements were computed as described by Jordi et al. (1995), taking into account errors in the instrumental magnitudes and errors in the transformation equations, through the r.m.s. residuals of standards stars. Final magnitude, colours and errors were obtained by averaging the individual measurements of each star using the internal error as a weight (Jordi et al. 1995, Rosselló et al. 1985). The final errors as a function of apparent visual magnitude are given in Fig. 1. No study of variability was performed.

Table 1. Log of the observations (n gives the number of observed frames)

Telescope	date	exposure time(s)					seeing(")	n
		<i>U</i>	<i>B</i>	<i>V</i>	<i>R</i>	<i>I</i>		
2.20 m CAHA	1992-10-24	900	600	300	100	200	1.2	3
1.52 m OAN	1993-12-12	2000	800	500	200	600	1.3	1
1.23 m CAHA	1994-12-09	2000	500	500	200	300	1.9	1
1.23 m CAHA	1994-12-10	2000	500	500	200	300	2.5	1
1.23 m CAHA	1994-12-11	2000	500	500	200	300	1.9	1

Table 2. Number of standard stars (*N*) and their r.m.s. residuals (σ)

Night	V_{B-V}		$B-V$		$U-B$		$V-R$		$V-I$		V_{V-R}	
	<i>N</i>	σ	<i>N</i>	σ	<i>N</i>	σ	<i>N</i>	σ	<i>N</i>	σ	<i>N</i>	σ
1992-10-24	18	0.042	19	0.030	16	0.036	20	0.059	18	0.040	17	0.030
1993-12-12	16	0.051	17	0.025	14	0.027	18	0.021	17	0.019	16	0.050
1994-12-09	19	0.028	19	0.028	17	0.035	20	0.021	19	0.021	19	0.028
1994-12-10	10	0.030	10	0.040	9	0.045	11	0.016	10	0.025	11	0.040
1994-12-11	18	0.021	20	0.012	17	0.054	20	0.015	19	0.023	19	0.022

The frame of 1994-12-09 was used as a master frame and the others were tied into it. Since the pixel size was 0.502 arcsec the observed stars cover an area of about $9.5' \times 9.5'$. An identification number was assigned to each star by increasing right ascension. Equatorial coordinates were obtained from the known PPM stars (Röser and Bastian, 1989) in the master frame, taking one of them as origin and fitting the equations

$$\begin{aligned} \Delta\alpha \cos \delta &= a_0 + a_1\Delta x + a_2\Delta y \\ \Delta\delta &= b_0 + b_1\Delta x + b_2\Delta y \end{aligned}$$

where Δ means the difference in the sense *star* minus *origin*. The coefficients resulting from the fitting show a good alignment of $+x$ coordinate with $+\alpha$ and of $+y$ with $+\delta$; the coefficients a_2 and b_1 were almost zero.

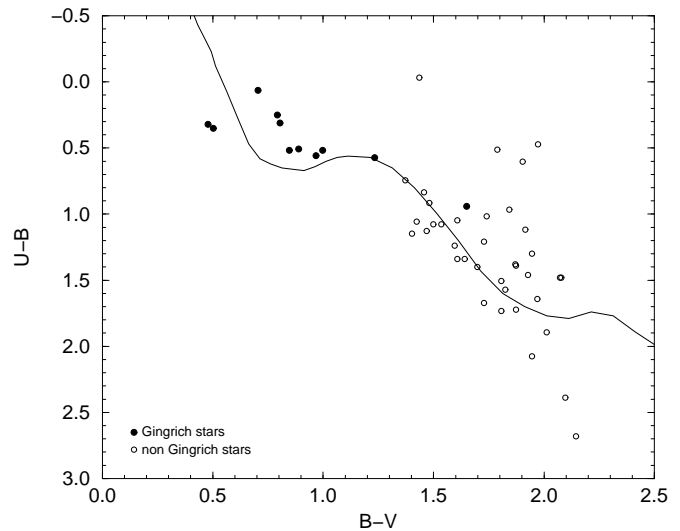
Table 3 gives *UBVRI* data for 123 stars down to visual magnitude 21. ($B-V$) colour was measured for 96 stars, ($U-B$) colour for 48, ($V-R$) colour for 122 and ($V-I$) colour for 120. Star centres are given as frame (x, y) and equatorial (α, δ) coordinates.

Observed stars were matched with IRAS PSC catalogue, Simbad Data Base and X-ray sources quoted in Preibisch et al. (1996). Cross identifications are given in Table 3 as notes. No matches were found with IRAS point sources. Quoted spectral types are from Černis (1993) and Simbad Data Base.

Following Jordi et al. (1995) we estimated our sample to be complete in $V, R,$ and I down to $V=18.5$ mag. However, due to the low detection of CCD cameras at short wavelengths, the completeness in the four colour indices is obtained only down to $V=15.5$ mag. Visual magnitude and four colour indices were determined for 48 stars (39% of the sample).

Colour-colour diagrams are shown in Figs. 2 and 3.

Harris et al. (1954), Strom et al. (1974) and Kwon & Lee (1983) obtained *UBV* photometry in the region. Černis (1993) also derived V magnitude from Vilnius photometry. Although there are few stars in common, we computed external photometric errors. Mean differences between previous photometric data and ours and the number of stars in common are shown in Table

**Fig. 2.** Observational colour-colour diagram. The solid line is the calibration by Schmidt-Kaler (1982) shifted by $E(B-V)=0.71$ and taken $E(U-B)/E(B-V)=0.837$

4. The greatest average difference and dispersion were found for the ($U-B$) colour, due to the difficulty of CCD measurements at short wavelengths and to the well-known homogeneity problems with this index (Bessel 1990).

3. Analysis of membership

Reddening makes the representative points of the stars on colour-colour diagrams move away from the standard calibrations. Jordi et al. (1996) described a suitable method to obtain individual reddening values from colour-colour diagrams by moving the standard calibrations step by step in a wide range of reddening values and finding the most probable ones. For each star, the method defines an adimensional value called proximity

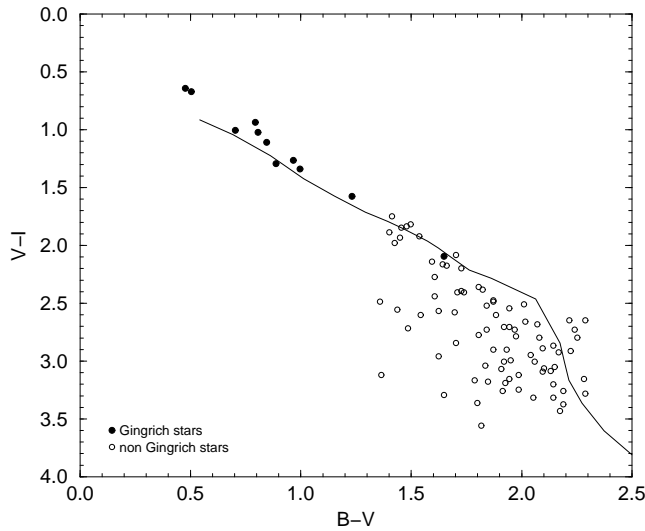


Fig. 3. Observational colour-colour diagram. The solid line is the calibration by Straižys (1992) shifted by $E(B-V)=0.71$ and taken $E(V-I)/E(B-V)=1.492$

Table 4. External errors: several authors - ours

	Harris et al. (1954) (11 stars)	Strom et al. (1974) (10 stars)
ΔV	$+0.001 \pm 0.030$	$+0.015 \pm 0.048$
$\Delta(B - V)$	-0.004 ± 0.009	-0.021 ± 0.019
$\Delta(U - B)$	$+0.053 \pm 0.086$	$+0.043 \pm 0.092$
	Kwon & Lee (1983) (11 stars)	Černis (1993) (13 stars)
ΔV	$+0.002 \pm 0.060$	-0.023 ± 0.056
$\Delta(B - V)$	-0.025 ± 0.025	-
$\Delta(U - B)$	$+0.032 \pm 0.114$	-

parameter d to each shifted calibration and looks for local minima, which we refer to as reddening solutions. Each reddening solution yields a value of $E(B-V)$ for the observed star and also its intrinsic colours $(B-V)_o$ and $(U-B)_o$ or $(V-I)_o$, depending on the observational plane. Due to the shape of the calibrations, more than one reddening solution could be found for a given star and then additional information would be needed in order to decide which of the reddening solutions is the most appropriate.

We applied the method to the observational plane $(B-V, U-B)$ ranging from $(B-V)_o = -0.33$ to $(B-V)_o = 1.64$. For the stars without observed $(U-B)$ colour we used the $(B-V, V-I)$ plane ranging from $(B-V)_o = 1.6$ to $(B-V)_o = 2.0$. For stars with $(B-V)_o < 1.6$ the reddening line is almost parallel to the calibration and the dereddening procedure gives unreliable solutions.

As standard calibration for the $(B-V, U-B)$ plane, we used the $[(B-V)_o, (U-B)_o]$ relation by Schmidt-Kaler (1982) for the ZAMS, fitted by a ten-degree polynomial. This calibration is rather similar to that by Mermilliod (1981) but it covers a wider range of colour indices, and it is very similar to that by Schmidt-

Kaler (1982) for luminosity class V. So, the derived individual reddening is independent of the calibration adopted. Each point of the calibration was reddened along a line whose slope was taken from Straižys (1992).

As standard calibration for the $(B-V, V-I)$ plane, we used the $[(B-V)_o, (V-I)_o]$ relation by Straižys (1992) fitted by an eight-degree polynomial. The slope of the reddening line was $E(V-I)/E(B-V)=1.492$ (Scheffler 1982).

We considered a colour excess interval of $-0.050 < E(B-V) < 4.000$ mag explored in steps of 0.001 mag, which includes the whole range of reddening values expected for IC 348. Negative values were introduced in order to take into account observational errors and cosmic dispersion for the stars close to the calibration lines. Reddening solutions with proximity parameter $d > 1$ were not taken into account thereafter.

Jordi et al. (1996) selected member candidates of Cepheus OB3 association by comparing the colour excess and the distance modulus of each reddening solution with the average values of the previously known members. Distance moduli in Cepheus OB3 were computed through a colour-absolute magnitude calibration $[(B-V)_o, M_v]$ for the ZAMS. The problem in IC 348 is slightly different because we have to take into account the presence of PMS stars already quoted by previous authors.

From our photometry we computed the average colour excess of the brightest known members of IC 348, obtaining a value of $E(B-V)=0.71 \pm 0.24$ mag. We accepted as preliminary candidate members those stars for which at least one reddening solution was available in a 2σ margin of this average value. Fig. 4a shows the location of the known members and the preliminary candidates in the $(V-R, V)$ colour-magnitude diagram. As dashed line we overplotted the absolute magnitude $[(V-I)_o, M_v]$ calibration by Reid & Gilmore (1982), for main sequence stars, transformed to a $[(V-R)_o, M_v]$ calibration using Straižys (1992), shifted by the average colour excess and absorption and assuming a distance to the cluster of 260 pc (Černis 1993). As can be seen, most of the preliminary candidates are placed above the relation for class V stars, the redder the star the greater the displacement. This confirms the presence of PMS stars and indicates that instead of looking for members around the ZAMS relation, they should be sought around an “observational isochrone” defined by the preliminary candidates. A fourth-degree polynomial was fitted to these preliminary candidates to compute the observational isochrone. It is drawn in Fig. 4a as solid line and we would remark that the stars identified as PMS stars in previous studies, are located very close to the observational isochrone. Those stars, from the whole sample of 123 observed stars, located inside a 3σ margin of the observational isochrone were accepted as candidate members. Analogously, the procedure was applied to the $(B-V, V)$ and $(V-I, V)$ planes (Figs. 4b and 4c) and those candidates in the three planes were finally accepted as members of the cluster (114 stars). They are labeled “M” in Table 3. They represent a group of stars with similar reddening and placed about the same distance from us. All of our observed stars that present

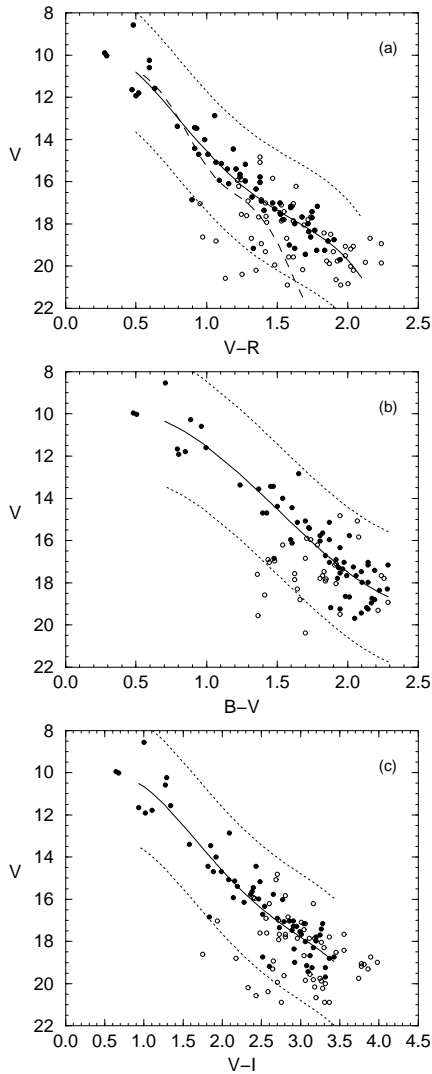


Fig. 4a–c. Observational colour-magnitude diagrams. Dashed line in **a** is the calibration by Reid & Gilmore (1982) for main sequence stars shifted by the average colour excess and absorption and assuming a distance of 260 pc. Filled circles are stars with at least one reddening solution compatible and open circles are stars with reddening solutions non compatible or without reddening solution (see text). Solid line are fits to preliminary candidate members ($\sigma_{V-R} = 0.947$, $\sigma_{B-V} = 1.029$, $\sigma_{V-I} = 1.001$) and dotted lines represent the acceptance margin of 3σ

H_{α} and/or X-ray emission (Preibisch et al., 1996) were classified as members by the described procedure.

For the brightest members, Table 5 indicates the individual colour excess, absorption (computed using the ratio of total-to-selective absorption by Straižys (1992) as a function of $(B-V)_o$) and the intrinsic colours. Appropriate reddening solution was selected from multiple solutions by comparison with the colour excess of the previously known neighbour members. The mean colour excess and visual absorption of stars listed in Table 5 are 0.85 ± 0.28 and 2.80 ± 0.93 mag, respectively.

The brightest previously known members are placed at a mean distance modulus of 6.90 ± 0.93 mag, i.e. 240 pc, using

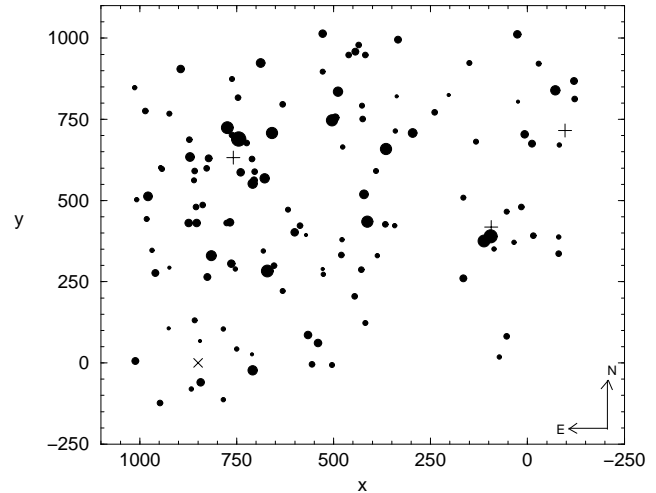


Fig. 5. Spatial distribution of the observed stars. Signs (+) correspond to the centres of the sub-clusters *a*, *h* and *i* of Lada & Lada (1995). Sign (x) shows the centre of the new visual sub-cluster identified in this work

the absolute magnitude calibration by Schmidt-Kaler (1982) (star number 93, already known to be a PMS star, was rejected since the absolute magnitude calibration is not suitable). This determination is in good agreement with that by Černis (1993). As the author used a larger sample than us to determine the cluster distance, we decided to adopt his determination of 260 ± 16 pc.

4. Discussion

4.1. Population and spatial distribution

The analysis of the membership yields a population of the cluster of 114 stars in the area studied, which represents 93% of the observed stars.

The cluster shows structure and noticeable inhomogeneities in reddening and absorption. The spatial distribution (Fig. 5) in our observed area roughly follows the *K* band star counts by Lada & Lada (1995). Our area corresponds mainly to their densest sub-cluster, *a*, and also includes sub-clusters *h* and *i*. With our passbands, the sub-cluster *i* is also relevant but the sub-cluster *h* is less evident due to the youth of the sub-cluster, giving few visual stars, or to deficiency of our sample, since this sub-cluster is placed at the edge of our field. Table 6 gives the stellar density of sub-cluster *a* as a function of the distance to its centre ($x \approx 750$, $y \approx 650$; $\alpha \approx 3^h 44^m 34^s$, $\delta \approx 32^{\circ} 9' 25''$). The surface density decreases approximately as r^{-1} , as found by McCaughrean & Stauffer (1994) in young embedded clusters. However, the central density is lower than that found by Lada & Lada (1995) in the *K* band. This may be due to the different passband used and the limiting magnitude of the observations. In contrast, the surface density of the sub-cluster *i* is found to be of the same value as Lada & Lada (1995). Because of the

Table 6. Surface stellar density in the sub-cluster *a* of IC 348

Radius (pc)	Number of stars	Density (stars pc ⁻²)	Number of members	Density (stars pc ⁻²)
0.08	13	647	12	597
0.16	31	385	30	373
0.24	50	276	49	271
0.32	74	230	71	221

presence of gas and dust, optical detection is less effective in region *a* than in region *i*.

At the south-east another sub-cluster appears that is not evident in the previous study. It is placed at ($x \approx 850$, $y \approx 0$; $\alpha \approx 3^h44^m38^s$, $\delta \approx 32^\circ3'57''$), with a radius of about 0.09 pc and a population of 12 stars (10 being assumed as members), giving a surface stellar density of 472 stars pc⁻², similar to that of the *i* sub-cluster.

4.2. Ages

Strom et al. (1974) estimated the age of the IC 348 open cluster to be about 5-20 10⁶ yr, while, from simulations, Lada & Lada (1995) derived continuous star formation over the last 5-7 10⁶ yr.

In computing ages in the present work, PMS tracks for low mass stars were taken from D'Antona & Mazzitelli (1994) using Alexander et al. (1989) and Rogers & Iglesias (1992) opacities, and the Canuto & Mazzitelli (1990) model for the stellar convection. Isochrones were derived in terms of luminosity and effective temperature from tracks of different stellar masses.

The isochrones were translated onto colour-magnitude diagram by means of Bohm-Vitense (1981) and Arribas & Martinez Roger (1988) to convert T_{eff} to $(B-V)_o$, Straižys (1992) to convert $(B-V)_o$ to $(V-R)_o$ or $(V-I)_o$ and Malagnini et al. (1986) to convert stellar luminosity to absolute magnitude. Mean colour excess and distance modulus from the previously known members (Gingrich's stars) were used to obtain the isochrones in the observational plane.

Once in the observational plane, $(V-R, V)$ for example, the distance of the star member j of the cluster to a given isochrone was computed as:

$$d_j^2 = \text{MIN}_{i=1, \dots, n} \left[\left(\frac{V_j - V_i}{\sigma_{V_j}} \right)^2 + \left(\frac{(V-R)_j - (V-R)_i}{\sigma_{(V-R)_j}} \right)^2 \right]$$

where V_i and $(V-R)_i$ are the different points of the isochrone given by different stellar masses.

Following Flannery & Johnson (1982), a mean distance of all member stars to the isochrone can be obtained by:

$$\Psi = \left(\sum_{j=1, \dots, N} d_j \right) / N$$

where N is the number of stars in the sample of members. On the assumption that all the stars have the same age, the minimum value of Ψ gives the most probably age of the cluster. Fig. 6 shows the computed Ψ as a function of the log age in the range

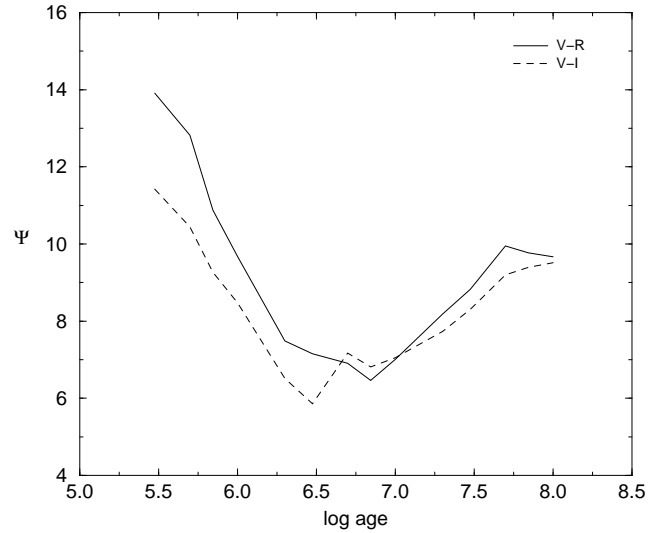


Fig. 6. Mean distance of members from each isochrone in the magnitude colour diagrams $(V-R, V)$ and $(V-I, V)$

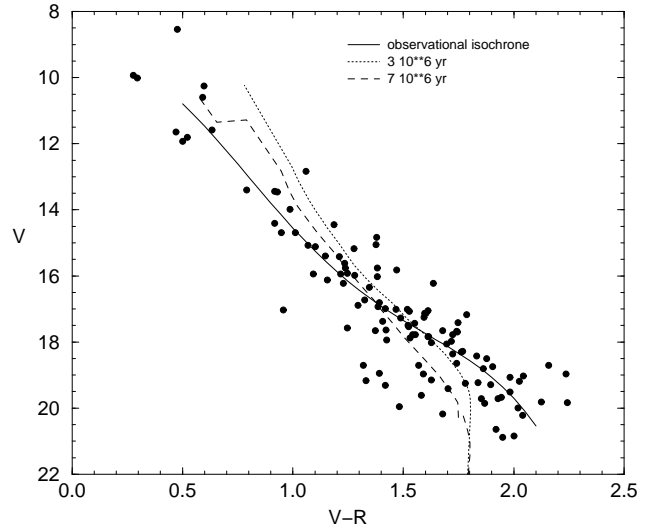


Fig. 7. Observational colour-magnitude diagram for the 114 accepted members of IC 348. Solid line is the “observational isochrone” (see text). Dashed and dotted lines correspond to the PMS isochrones of D’Antona & Mazzitelli (1994) with CM model for stellar convection, shifted by the average colour excess and absorption and assuming a distance of 260 pc

of 3 10⁵ and 10⁸ yr as derived from the observational planes $(V-R, V)$ and $(V-I, V)$. Uncertainties in the transformations and different observational errors may explain the slight difference in the two minima. From the figure an age of 3-7 10⁶ yr for IC 348 is derived. This result is compatible with the age quoted by Strom et al. (1974). However, the rather high value of Ψ could indicate the presence of a significant spread of ages and the assumption that all the stars have the same age may not be valid, as pointed out by Lada & Lada (1995).

Fig. 7 shows the colour-magnitude diagram of the sample of 114 stars accepted as members of IC 348, with the isochrones of $3 \cdot 10^6$ and $7 \cdot 10^6$ yr. The “observational isochrone” as fitted in Sect. 3 is overplotted for reference.

5. Conclusions

Deep *UBVRI*-CCD photometry for 123 stars, down to apparent visual magnitude 21, in the central region of IC 348 open cluster was obtained. Colour-colour and colour-magnitude diagrams allow us to classify 114 of the observed stars as members of the cluster on the basis of similar colour excess and distance. For the brightest members, we give the computed individual reddening. A strong variation of the colour excess over the field is found, so large inhomogeneities in the distribution of the interstellar medium can be deduced.

The decrease in the stellar surface density towards the outer regions of the cluster as a whole, and the sub-clustering agree rather well with *JHK* studies by Lada & Lada (1995). A new visual sub-cluster at the south of the densest concentration (sub-cluster *a*) has been identified, with a surface stellar density similar to other sub-clusters in the field.

Our colour-magnitude diagrams indicate a large population of PMS stars, some of them already identified as PMS by previous authors (by their H_α emission).

From recent PMS evolutionary models for low mass stars, we derived an age of $3\text{--}7 \cdot 10^6$ yr for the cluster, which is compatible with previous estimations of the age. There are indications, however, that a continuous star formation model may be more reliable than a coeval model.

Acknowledgements. We thank I. Ribas for his kind collaboration in the reduction of data. We also thank J.M. Paredes, D. Galadí-Enríquez and I. Ribas for their collaboration in the observations. We appreciate the constructive comments by our anonymous referee. The 1.23 m and 2.20 m telescopes are operated by the Max-Planck Institut für Astronomie at Calar Alto Observatory of the Centro Astronómico Hispano-Alemán. The 1.52 m telescope is operated by the Observatorio Astronómico Nacional at Calar Alto Observatory of the Centro Astronómico Hispano-Alemán. This work was supported by the CICYT under contract ESP95-0180, and by the *Ayudas para la utilización de recursos científicos de carácter específico* by the DGICYT.

References

Alexander D.R., Augason C.G., Johnson H.R., 1989, *ApJ* 345, 1014
 Arribas S., Martínez Roger, C., 1988, *A&A* 206, 63
 Bachiller R., Cernicharo J., 1986, *A&A* 166, 283
 Bachiller R., Guilloteau S., Kahane C., 1987, *A&A* 173, 324
 Bessel M.S., 1990, *PASP* 102, 1181
 Blaauw A., 1952, *Bull. Astron. Inst. of Netherlands* 11, 405
 Bohm-Vitense E., 1981, *ARAA* 19, 295
 Canuto V.M., Mazzitelli I., 1990, *ApJ* 370, 295
 Černis K., 1993, *Baltic Astronomy* 2, 214
 D’Antona F., Mazzitelli I., 1994, *ApJS* 90, 467
 Flannery B.P., Johnson B.C., 1982, *AJ* 263, 166
 Galadí-Enríquez D., Jordi C., Trullols E., 1994, in *New Developments in Array Technology and Applications*, ed. A.G.D. Philip (Proc. IAU Symp. 167), p. 327

Gingrich C.H., 1922, *ApJ* 56, 139
 Greenstein J.L., 1948, *ApJ* 107, 376
 Harris D.L., Morgan W.W., Roman N.G., 1954 *ApJ* 119, 622
 Herbig G.H., 1954, *PASP* 66, 19
 Hubble E., 1922, *ApJ* 56, 162
 Jordi C., Galadí-Enríquez D., Trullols E., Lahulla F., 1995, *A&AS* 114, 1
 Jordi C., Trullols E., Galadí-Enríquez D., 1996, *A&A* 312, 499
 Lada C.J., 1994, in *The Cold Universe*, eds. T. Montmerle, C.J. Lada, F. Mirabel, J.T.T. Van, Dordrecht, Reidel, p. 211
 Lada E.A., De Poy D.L., Evans N.J., Gatley I., 1991, *ApJ* 371, 171
 Lada E.A., Lada C.J., 1995, *AJ* 109, 1682
 Ladd E.F., Lada E.A. Myers P.C., 1993, *ApJ* 410, 168
 Landolt A.U., 1983, *AJ* 88, 439
 Landolt A.U., 1992, *AJ* 104, 340
 Malagnini M.L., Morossi C., Rossi L., Kurucz R.L., 1986, *A&A* 162, 140
 McCaughrean M.J., Stauffer J.R., 1994, *AJ* 108, 1382
 Mermilliod J.-C. 1981, *A&A* 97, 235
 Kwon S.M., Lee S.-W., 1983, *J. Korean Astron. Soc.* 16, 7
 Preibisch Th., Zinnecker H., Herbig G.H. 1996, *A&A* 310, 456
 Reid N., Gilmore G., 1982, *MNRAS* 201, 73
 Rogers F.J., Iglesias C.A., 1992, *ApJS* 79, 507
 Röser S., Bastian U., 1989, *PPM-positions and proper motions-North*, Astron. Rechen. Inst. Heidelberg
 Rosselló G., Calafat R., Figueras F., et al., 1985, *A&AS* 59, 399
 Sancisi R., Goss W.M., Anderson C., Johansson L.E.B., Winneberg A., 1974, *A&A* 35, 445
 Scheffler H., 1982, in *Landolt-Börnstein, New Series, Group II, Vol. 2, Subvol. C*, Springer-Verlag, Berlin
 Schmidt-Kaler Th., 1982, in *Landolt-Börnstein, New Series, Group VI, Vol. 2, Subvol. B*, Springer-Verlag, Berlin
 Stetson P.B., 1987, *PASP* 99, 191
 Stetson P.B., 1990, *PASP* 102, 932
 Stetson P.B., 1993, *Proc. IAU Coll. 136*. Cambridge University Press, Cambridge, p. 291
 Straižys V., 1992, *Multicolor Stellar Photometry*. Pachart Publishing House, Tucson
 Strom S.E., Strom K.M., Carrasco L., 1974, *PASP* 86, 798